Construction and photophysics study of supramolecular complexes composed of three-point binding fullerene–trispyridylporphyrin dyads and zinc porphyrin

ARTICLE *in* PHYSICAL CHEMISTRY CHEMICAL PHYSICS · NOVEMBER 2010

Impact Factor: 4.49 · DOI: 10.1039/c0cp01076f · Source: PubMed

Construction and photophysics study of supramolecular complexes composed of three-point binding fullerene-trispyridylporphyrin dyads and zinc porphyrin†

Wei Xu,[ab] Lai Feng,[a] Yishi Wu,[a] Taishan Wang,[ab] Jingyi Wu,[ab] Junfeng Xiang,[a] Bao Li,[ab] Li Jiang,[a] Chunying Shu*[a] and Chunru Wang*[a]

Received 5th July 2010, Accepted 22nd October 2010
DOI: 10.1039/c0cp01076f

A series of novel supramolecular complexes composed of a three-point binding C_{60}-trispyridylporphyrin dyad (1) or C_{70}-trispyridylporphyrin dyad (2) and zinc tetraphenylporphyrin (ZnP) were constructed by adopting a "covalent–coordinate" bonding approach, composed of three-point binding. The dyads and self-assembled supramolecular triads or pentads formed by coordinating the pyridine groups located on the dyads to ZnP, have been characterized by means of spectral and electrochemical techniques. The formation constants of ZnP-1 and ZnP-2 complexes were calculated as 1.4×10^4 M^{-1} and 2.0×10^4 M^{-1}, respectively, and the Stern–Volmer quenching constants K_{SV} were founded to be 2.9×10^4 M^{-1} and 5.5×10^4 M^{-1}, respectively, which are much higher than those of other supramolecular complexes such as previously reported ZnP-3 (*N*-ethyl-2-(4-pyridyl)-3,4-fulleropyrrolidine). The electrochemical investigations of these complexes suggest weak interactions between the constituents in the ground state. The excited states of the complexes were further monitored by time-resolved fluorescence measurements. The results revealed that the presence of the multiple binding point dyads (1 or 2) slightly accelerated the fluorescence decay of ZnP in *o*-DCB relative to that of the "single-point" bound supramolecular complex ZnP-3. In comparison with 1 and 2, C_{70} is suggested as a better electron acceptor relative to C_{60}. DFT calculations on a model of supramolecular complex ZnP-1 (with one ZnP entity) were performed. The results revealed that the lowest unoccupied molecular orbital (LUMO) is mainly located on the fullerene cage, while the highest occupied molecular orbital (HOMO) is mainly located on the ZnP macrocycle ring, predicting the formation of radical ion pair $ZnP^{+\bullet}$-H_2P-$C_{60}^{-\bullet}$ during photo-induced reaction.

Introduction

Over the past decades, mimicking photosynthetic functions *via* synthetic model compounds has been of great interests for the purpose of solar energy conversion and construction of molecular optoelectronics.[1–7] One of the important characteristics of natural photosynthetic reaction centers is assembly of different photo- and redox-active components *via* noncovalent interactions. In which fullerene-porphyrin complexes play important roles due to their rich redox properties and extensive light absorption features.[8–21] In general, fullerenes are usually taken as electron acceptors due to their unique three dimensional aromatic structures which induce only small reorganization energy in electron transfer reactions,[3,22–32] and porphyrins are taken as electron donors because their wide light absorption range guarantees the efficient use of the solar spectrum. Experimentally, charge-separated states were always observed for various fullerene-porphyrin hybrids, which strongly suggests that there are photo-induced electron transfer reactions between fullerene and porphyrin moieties.

In order to achieve long-lived charge-separated states during photoinduced electron transfer processes, multi-step electron transfer reactions along well-defined redox gradients such as triads, tetrads, pentads, *etc*., were the most frequently used strategies. Until now, most reported fullerene-porphyrin hybrids have been in the non-covalently assembled multi-modular donor (D)-acceptor (A) form,[33] where usually one or more porphyrin moieties were assembled with a fullerene moiety by various non-covalent binding mechanisms such as metal-nitride coordination,[34–38] hydrogen bonding,[39–41] π–π stacking interactions,[42] and electrostatic interactions *etc*.[43] Since fullerenes as the reduction center of an electron transfer reaction can reversibly accept a number of electrons, the incorporation of multiple donors is expected to enhance the efficiency of intermolecular charge transfers.

Herein, we report the construction of a new multi-modular D-A system, (*n*-ZnP)-H2P-fullerene ($n > 1.5$), in which a free base porphyrin group is covalently linked with fullerene (*i.e*., C_{60} or C_{70}) and its three pyridyl groups can coordinate with more than one ZnP entity (Scheme 1). The alignment

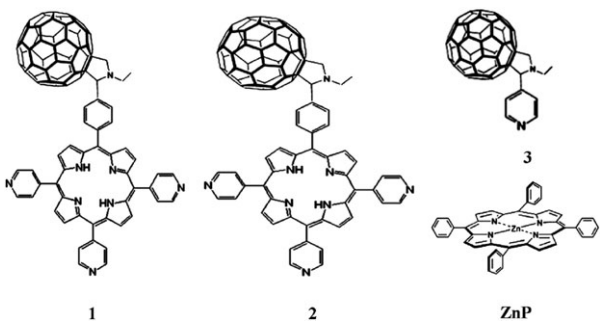

Scheme 1 Structures of C_{60}-trispyridylporphyrin dyad (**1**), C_{70}-trispyridylporphyrin dyad (**2**), *N*-ethyl-2-(4-pyridyl)-3,4-fulleropyrrolidine (**3**), and zinc tetraphenylporphyrin (ZnP).

[a] *Beijing National Laboratory for Molecular Sciences, Key Laboratory of Molecular Nanostructure and Nanotechnology, Institute of Chemistry, Chinese Academy of Sciences, Beijing 100190, China. E-mail: crwang@iccas.ac.cn*
[b] *Graduate School of CAS, Beijing 100049, China*

† Electronic supplementary information (ESI) available: Details for synthesis, characterization and time-resolved fluorescence spectra of the supramolecular complexes. See DOI: 10.1039/c0cp01076f

arrangement of multiple donors and acceptor agrees well with the gradient redox potentials of the complexes, and is expected to facilitate the multi-step photo-induced electron-transfer process.

Experimental section

Chemicals

C_{60} and C_{70} were synthesized by arc-discharge graphite under a helium atmosphere and isolated by high performance liquid chromatography (HPLC). Terephthalaldehydic acid methyl ester, pyridine-4-aldehyde, $LiAlH_4$, $(COCl)_2$ and *N*-ethyl-glycine were purchased from Alfa Aesar and used as received. All the solvents were dried prior to use. Free-base porphyrin/fullerene complex (**1**) was synthesized according to the literature.[44,45] And complex (**2**) was obtained by the same procedure; however, as suggested by the ^{1}H NMR studies, its mono-adduct includes three isomers, consistent with the previously reported 1,3-dipolar cycloaddition products of C_{70}.[46] Since the stabilities and electronic properties of the three isomers of **2** have been proved to be nearly identical, the isomeric mixture of **2** is used here as electron acceptor. Fulleropyrrolidine **3** was synthesized according to the literature.[47a] All the compounds were characterized using matrix-assisted laser desorption/ionisation-time of flight mass (MALDI-TOF) spectrometry and ^{1}H NMR spectrometry.

Spectroscopic characterization

The HPLC isolations of C_{60} and C_{70} were performed on an LC-908 (Japan Analytical Industry Co., Ltd.) monitored by a UV detector at 310 nm. The UV-Vis absorption spectra were measured in Ortho Dichlorobenzene(*o*-DCB) using a UV-4802H spectrophotometer. NMR spectra were obtained using a Bruker Advance 400 or a Bruker Advance 600 spectrometer. MALDI-TOF mass spectra were obtained uaing a Bruker BIFLEX III mass spectrometer. Steady-state fluorescence emission spectra were recorded on a Cary Eclipse spectrometer in *o*-DCB. The fluorescence lifetimes were measured by a single-photo counting method using the second harmonic generation (SHG, 410 nm) of a Ti:sapphire laser (Tsunami) with a streak scope. The electrochemical measurements were performed in *o*-DCB using 0.05 M $(n\text{-}C_4H_9)_4NPF_6$ as supporting electrolyte. Cyclic voltammetry experiments were performed on a CHI660C Electrochemical Workstation with a three-electrode cell. The glassy carbon electrode and platinum plate were used as the working electrode and the counter electrode, respectively, and a saturated calomel reference electrode (SCE) was used as the reference electrode. The CV scan rate was set at 100 mV s^{-1}.

Calculations

The molecular geometry and electronic structure of complex ZnP-**1** were calculated using the MS dmol package[52] at the GGA-PBE/DNP level.

Results and discussion

Optical absorption and ^{1}H NMR studies

The UV-Visible absorption spectra of **1** and **2** in *o*-DCB exhibit typical characteristics of the free base porphyrin moiety (Fig. 1). Note that the molar absorption coefficients of their Soret bands are much lower than that of 5-(4-formylphenyl)-10,15,20-tris(4-pyridyl)porphine(H_2P), indicating a partial migration of electron density from the porphyrin ring towards the fullerene entity. Furthermore, the Soret band of **2** is more favorable to be quenched relative to that of **1**, indicative of more considerable conjugation between the two chromophores of **2**. Herein, the pyrolidine ring in **1** or **2** not only combines the free base porphyrin and fullerene moieties together but also functions as a space linker of charge transfer.[48a]

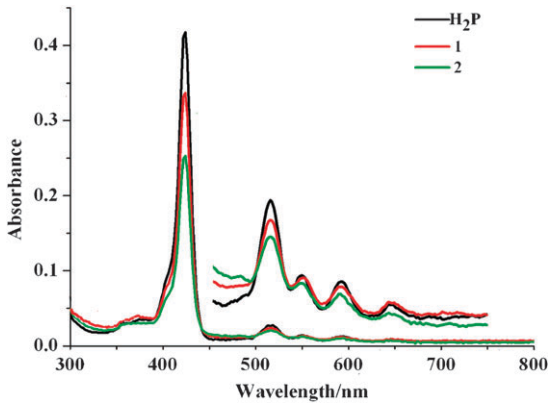

Fig. 1 UV-Visible absorption spectra of **1**, **2** and H_2P in *o*- DCB. All the compounds are at the same concentration of 2.5 μM. The inset shows the enlarged Q-band pattern.

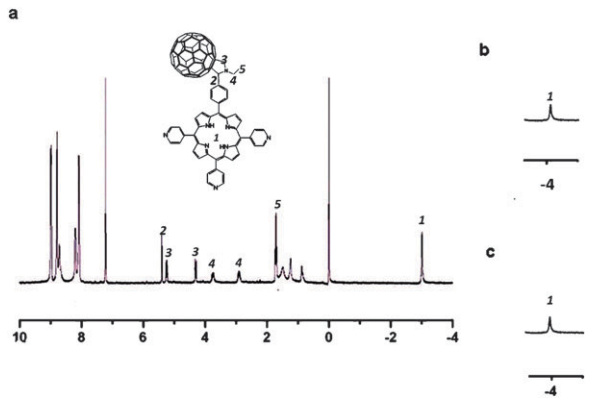

Fig. 2 ^{1}H-NMR spectra of **1** (a), and in the presence of 1.0 (b), 2.0 (c) equivalent of ZnP (400 MHz, $CDCl_3/CS_2$ = 2 : 1, ppm).

A ^{1}H NMR spectroscopic study of **1** in the absence or presence of ZnP was performed in $CDCl_3/CS_2$ (v : v = 2 : 1). As shown in Fig. 2, the chemical shift of internal pyrrolic protons of **1** undergoes *ca.* 0.3 ppm and 0.9 ppm up-field shifts upon one and two equivalent additions of ZnP as compared with that of the pristine **1** (*i.e.*, −3.0 ppm). Since the up-field shift of the internal pyrrolic protons along with the additions of ZnP might be derived from an electron deficiency on the porphyrin moiety of **1**, the NMR study unambiguously implies that there are intermolecular charge-transfer interactions between ZnP and **1**.

Table 1 Redox Potentials (V *vs.* Fc/Fc^{+}) of the self-assembled complexes of ZnP-**1** and ZnP-**2** in *o*-DCB, 0.05 M $(n\text{-}C_4H_9)_4NPF_6$

	$ZnP^{0/+}$	$\mathbf{1}^{0/-1}$ or $\mathbf{2}^{0/-1}$	$\mathbf{1}^{-1/-2}$ or $\mathbf{2}^{-1/-2}$	$ZnP^{0/-1}$
ZnP	0.26	—	—	−2.09
1	—	−1.33	−1.77	—
2	—	−1.27	−1.68	—
ZnP-**1** (0.4)	0.29	−1.25	−1.65	—
ZnP-**1** (0.8)	0.28	−1.24	−1.65	—
ZnP-**1** (1.6)	0.28	−1.23	−1.63	—
ZnP-**2** (0.4)	0.29	−1.09	−1.46	—
ZnP-**2** (0.8)	0.28	−1.09	−1.45	—
ZnP-**2** (1.6)	0.27	−1.08	−1.47	—

Electrochemical studies

To investigate the redox behaviors of ZnP-**1** and ZnP-**2**, electrochemical studies were performed using cyclic voltammetry (CV) in *o*-DCB with 0.05 M $(n\text{-}C_4H_9)_4NPF_6$ as supporting electrolyte. As shown in Table 1, along with the increased addition of **1** or **2** from 0.4, 0.8 to 1.6 equivalent of ZnP, the first oxidation potential of ZnP was found to have a 20–30 mV anodic shift (correspondingly at 0.29/0.29, 0.28/0.28 and 0.28/0.27 V, respectively) relative to that of pristine ZnP (0.26 V). Detailed CV studies are shown in Fig. S6 of the ESI†. The first and the second reduction potentials of the complex ZnP-**1** (with 0.4 equivalent of **1**) were observed at −1.25 V and −1.65 V, respectively, which should be derived from the C_{60} moiety of **1**. Along with the increased addition of **1**, there are also 10–20 mV anodic shifts of the reductive potentials. Similar results were observed for the complex of ZnP-**2**. Therefore, the very weak charge transfer interactions between ZnP and fullerene-trispyridylporphyrin dyads (**1** or **2**) in the supermolecular complexes are suggested.[48b]

Steady-state fluorescence emission studies

The photochemical behavior of all the three supermolecular complexes was investigated by using steady-state titration experiments. On addition of compounds **1**, **2** or **3** to an *o*-DCB solution of ZnP, the fluorescence intensity of the ZnP decreased. As shown in Fig. 3 (a), with the increased addition of **1** to ZnP in *o*-DCB, the steady state fluorescence of ZnP was transfered from the excited singlet state of ZnP to **1** at 550 nm excitation, which in turn confirms the formation of supramolecular complex. The complexation of ZnP with **1** in solution was determined by means of Job's plot based on the fluorescence intensity change at 597 nm. Fig. 3 (a) (inset) shows that a continuous variation plot of fluorescence intensity *versus* [ZnP]/([ZnP]+[**1**]) in *o*-DCB gave a maxial value of 0.64, indicating the formation of ZnP-**1** complex with a coordination ratio at 1.7 : 1. The binding constant, K_a, for the supramolecular complex formation evaluated by the modified Benesi–Hidebrand analysis and plots,[47b] is 1.4×10^4 M^{-1}(Fig. 3 (b)).The Stern–Volmer plot[47c] constructed from the fluorescence quenching data is shown in Fig. 3 (c). The Stern–Volmer quenching constant, K_{SV} calculated from the linear segment of the plots was found to be 2.9×10^4 M^{-1}. The similar quenching behavior of ZnP-**2** was observed as shown in Fig. 4 (a), and the complex formation 2.1 : 1 for ZnP-**2** was suggested by means of Job's plot (Fig. 4 (a) inset). By Benesi–Hildebrand analysis of the fluorescence data,

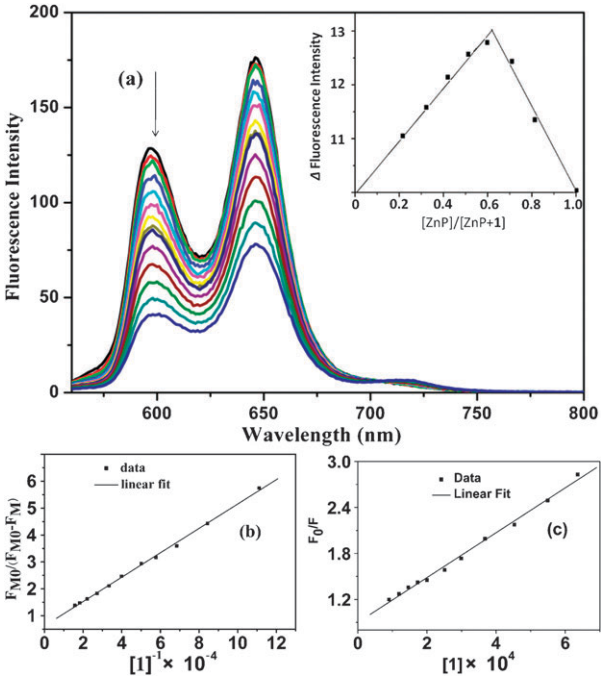

Fig. 3 (a) Steady-state fluorescence spectra of ZnP (2.6×10^{-5} M) with the increasing addition of **1** in *o*-DCB. Inset shows Job's plot at 597 nm. The total concentration of **1**+ZnP was maintained constant at 5.0×10^{-5} M. λ_{ex} = 550 nm. (b) Benesi–Hidebrand analysis of the fluorescence data. (c) Stern–Volmer plots for the fluorescence quenching of ZnP at 597 nm by **1**.

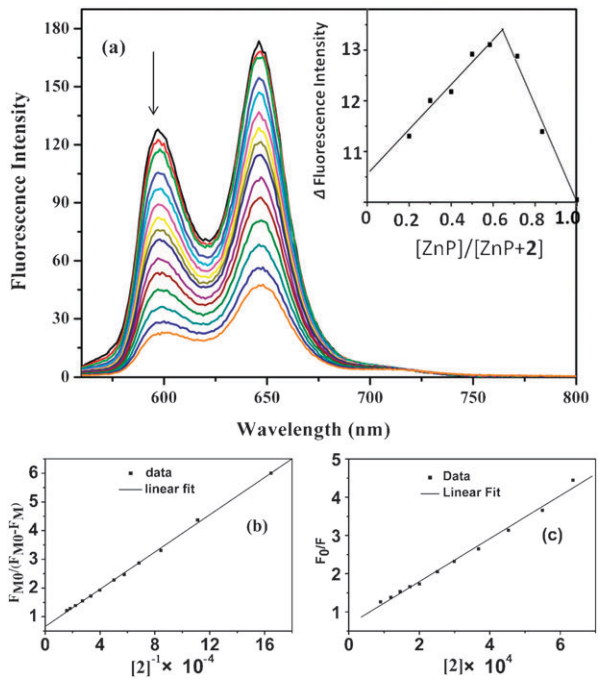

Fig. 4 (a) Steady-state fluorescence spectra of ZnP(2.6×10^{-5} M) with the increasing addition of **2**($0.61–6.36 \times 10^{-5}$ M) in *o*-DCB. Inset shows Job's plot at 597 nm. The total concentration of **2**+ZnP was maintained constant at 5.0×10^{-5} M. λ_{ex} = 550 nm. (b) Benesi–Hidebrand analysis of the fluorescence data. (c) Stern–Volmer plots for the fluorescence quenching of ZnP at 597 nm by **2**.

K_a = 2.0 × 10^4 M^{-1} was calculated (Fig. 4 (b)), and the Stern–Volmer quenching constant (K_{SV}) was calculated to be 5.5 × 10^4 M^{-1} (Fig. 4 (c)). For comparison, the calculated binding constant K_a is 6.0 × 10^3 M^{-1}, the Stern–Volmer quenching constants K_{SV} is 9.9 × 10^3 M^{-1}, and the corresponding complex formation is 1.0 : 1 for ZnP-**3** (Fig. S7 of the ESI†).

The results suggest the higher stability of the "three-point" bound supramolecular complexes ZnP-**1** and ZnP-**2**, and the efficiency of quenching was much higher than that of the "single-point" bound complex ZnP-**3**. Though there is a three-point motif of **1** and **2** for the formation of supramolecular complexes, the actual coordinated number of ZnP is less than two, much less than the binding sites on free-base porphyrin due to the spatial hindrance.

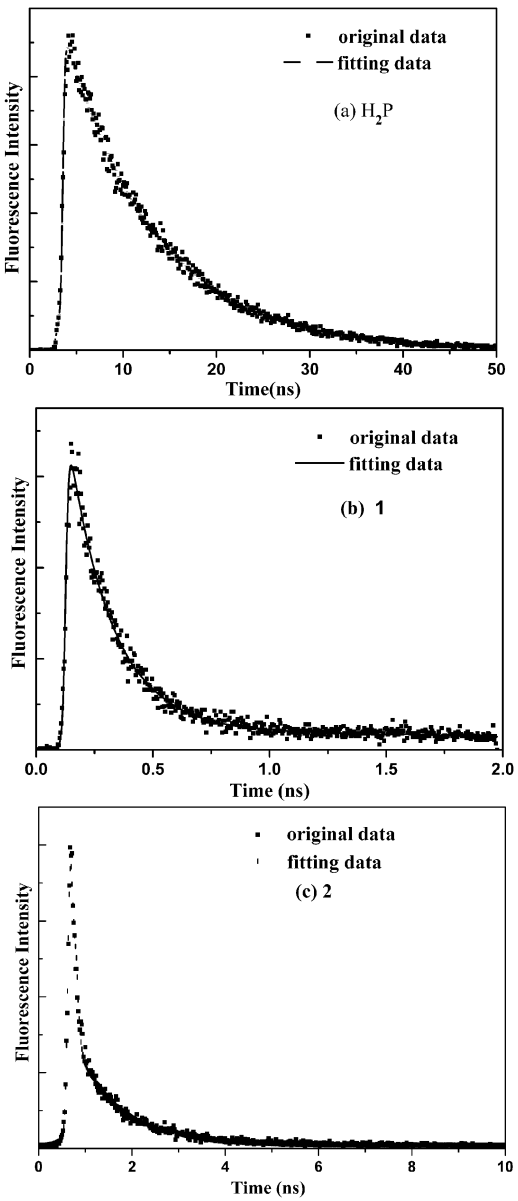

Fig. 5 Fluorescence decay profiles of (a) H_2P (~0.04 mM) (b) **1** (~0.04 mM) and (c) **2** (~0.04 mM) in *o*-DCB, λ_{em} = 410 nm.

Table 2 Fluorescence Lifetimes (τ_f), charge-separation rate constants (κ_{cs}), charge-separation quantum yields (Φ_{cs}) of the dyads and supramolecular triads in *o*-DCB

Compound	λ_{em}, nm	τ_f/ps	κ_{cs}/s^{-1}	Φ_{cs}
H_2P	650–730	9217	—	—
1	650–730	181 (τ_{f1}) 3294 (τ_{f2})	5.41 × 10^9	0.98
2	650–730	44 (τ_{f1}) 949 (τ_{f2})	2.25 × 10^{10}	0.9995
ZnP	590–670	1875	—	—
ZnP + **3** (1 : 1)	590–670	1873	4.38 × 10^5	0.0008
ZnP + **3** (1 : 3)	590–670	1849	7.32 × 10^6	0.0135
ZnP + **1** (1 : 1)	590–670	1840	9.98 × 10^6	0.02
ZnP + **1** (1 : 3)	590–670	1790	2.50 × 10^7	0.045
ZnP + **2** (1 : 1)	590–670	1810	1.89 × 10^7	0.034
ZnP + **2** (1 : 3)	590–670	1774	3.04 × 10^7	0.054

$K_{CS} = (1/\tau_f)_{sample} - (1/\tau_f)_{ref}$; $\Phi_{cs} = [(1/\tau_f)_{sample} - (1/\tau_f)_{ref}]/(1/\tau_f)_{sample}$; [ZnP] = 0.04 mM in *o*-DCB, λ_{em} = 410 nm.

Picosecond time-resolved fluorescence studies

The fluorescence decay processes of **1**, **2** and H_2P in *o*-DCB were monitored in the range of 650–730 nm with excitation at 410 nm (Fig. 5). The time profiles exhibited a biexponential decay process deriving from a combination of an ultrafast decay component and a comparatively longer decay component. The faster decays (τ_{f1}) of **1** and **2** were evaluated as *ca.* 181 ps and 44 ps, respectively; whereas the corresponding longer decays (τ_{f2}) were 3300 ps and 950 ps, respectively, much shorter than that of H_2P (9217 ps). These results indicate an occurrence of an electron transfer or an energy transfer process between the H_2P moiety and fullerene moiety.[49] The evaluated fluorescence lifetimes (τ_f), the charge-separated rates (k_{cs}) and the quantum yields (Φ_{cs}) are summarized in Table 2. In particular, the faster decay components of **1** and **2** might be assigned to the decay of excited H_2P moiety as a result of electron transfer from it to fullerene moiety.[50] The longer decay components of **1** and **2** are probably induced by the singlet–singlet energy transfer from $^1H_2P^*$ to C_{60} or C_{70}.[51] It should be noted that the fluorescence decays of **2** was much faster than that of **1**, suggesting that C_{70} is a better electron acceptor relative to C_{60}. Furthermore, the fluorescence decays (τ_f) of ZnP in the presence of various amount of **1**, **2** and **3** in *o*-DCB were measured with excitation at 410 nm, and monitored in the region of 590–670 nm. All the time profiles of these complexes could be fitted as a monoexponential decay process. In the presence of equal or excess amount of **1** or **2**, summarized in Table 2. components of **1** and **2** might be attributed to the reduction in fluorescence decay time of ZnP being slightly accelerated as compared with that of ZnP in ZnP-**3** system (Fig. S8–S10 of the ESI†), which also suggested that the increased coordination number can contribute to the short fluorescence lifetime.

Computational studies

To visualize the molecular geometry and electronic structure of the complexes, computational studies were performed at the GGA-PBE/DNP level using the MS dmol package.[52] Three different binding sites (*a*, *b* and *c*) of ZnP-**1**(1 : 1) were

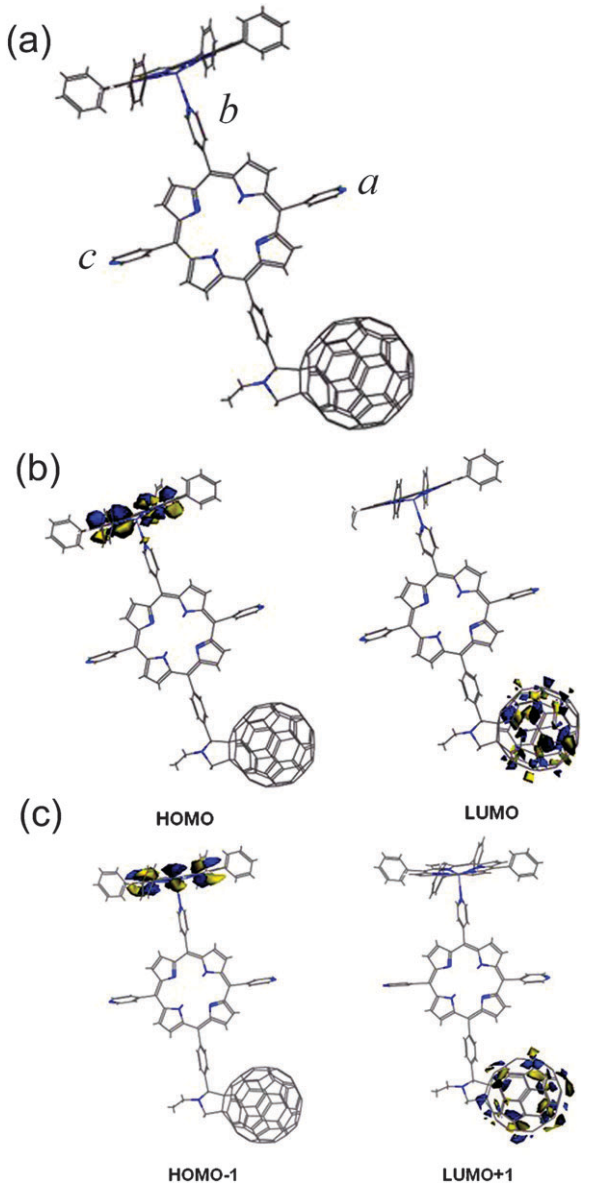

Fig. 6 Optimized structure of the triad B (a), optimized frontier HOMO and LUMO (b), HOMO-1 and LUMO + 1 (c) of the supramolecular complex. (*a*, *b* and *c* refer to the different binding sites).

optimized on a Born–Oppenheimer potential energy surface, and the global minima for each complex were obtained. The optimized structure and the PBE/DNP-generated frontier highest occupied molecular orbital (HOMO) and lowest unoccupied molecular orbital (LUMO) for binding site *a* are shown in Fig. 6. Obviously, the LUMO and LUMO + 1 were located on the fullerene cage, while the HOMO and HOMO-1 were dominantly located on the ZnP macrocycle ring (Fig. 6 (b) and (c)). These results suggest weak or negligible charge-transfer interactions between ZnP and fullerene dyad in the ground state, agreeing reasonably with the electrochemical results. The locations of the HOMO and LUMO also predict the formation of a $ZnP^{\bullet+}$-$C_{60}^{\bullet-}$ charge-separated state during photo-induced electron transfer reaction. The optimized relative energies of three different complexes of ZnP-**1** as well as their Zn–N bond lengths and the Mulliken charges of the Zn atom are summarized in Table 3. Among them, the complex B with ZnP coordinating on site *b* has the lowest energy, while the others coordinating on site *a* or *c* slightly higher energies. These results suggest that in the complex ZnP-**1**, ZnP prefers to coordinate *para* to the C_{60} *via* the free base porphyrin moiety. As a result, ZnP, free base porphyrin and C_{60} moieties have a tendency to be linearly arranged during the complex formation.

Table 3 Optimized relative energy, bond lengths of Zn–N (Pyridine) and Mulliken charge of Zn for the complexes of ZnP-**1**(1 : 1) at GGA-PBE/DNP Level

Complexes of **1** : ZnP	Binding point	Relative energy (kCal·mol^{-})	R_{Zn-N}/Å	Mulliken charge (Zn)
Complex A	*a*	4.51	2.254	0.758
Complex B	*b*	0	2.272	0.764
Complex C	*c*	5.22	2.279	0.762

Conclusions

We have demonstrated the formation of the supramolecular complexes (*n*-ZnP)-**1** and (*n*-ZnP)-**2** ($n > 1.5$) *via* coordination of the "three-point" binding fulleropyrrolidine with ZnP. The binding constants and the Stern–Volmer quenching constants were evaluated using steady-state fluorescence titration experiments, and are higher than that of other supramolecular complex with only "one-point" axial coordination (*i.e.*, ZnP-**3**). Job's plot based on the fluorescence intensity changes revealed the formation of ZnP : 1 and ZnP : 2 complexes with coordinating ratio at 1.7 : 1 and 2.1 : 1 between the ZnP-donor and the fulleropyrrolidine entities-acceptor (*i.e.*, **1** and **2**), respectively. The results of the time-resolved fluorescence decay studies on complexes (*i.e.*, ZnP-**1**, ZnP-**2** and ZnP-**3**) revealed that increasing the binding points of fulleropyrrolidine entities slightly accelerates the fluorescence decay of ZnP, indicating the predominance of **1** or **2** as electron acceptors. The theoretical calculations on the complexes of ZnP-**1** (1 : 1) further revealed the separated HOMO and LUMO distributions on ZnP and C_{60} moiety of **1**, respectively, predicting the formation of radical ion pair $ZnP^{+\bullet}$-H_2P-$C_{60}^{-\bullet}$ during the photo-induced electron transfer process.

Acknowledgements

This work is supported by the National Natural Science Foundation of China (No. 20702053), CMS-CX200913, 973 Program (No. 2006CB300402) and Important National Science & Technology Specific Projects (2008ZX05013-004).

References

1 M. R. Wasielewski, *Chem. Rev.*, 1992, **92**, 435–461.
2 A. P. de Silva, H. Q. N. Gunaratne, T. Gunnlaugsson, A. J. M. Huxley, C. P. McCoy, J. T. Rademacher and T. E. Rice, *Chem. Rev.*, 1997, **97**, 1515–1566.
3 H. Kurreck and M. Huber, *Angew. Chem., Int. Ed. Engl.*, 1995, **34**, 849–866.
4 D. Gust, T. A. Moore and A. L. Moore, *Acc. Chem. Res.*, 2001, **34**, 40–48.
5 D. M. Guldi, *Chem. Soc. Rev.*, 2002, **31**, 22–36.

6 C. J. Brabec, N. S. Sariciftci and J. C. Hummelen, *Adv. Funct. Mater.*, 2001, **11**, 15–26.
7 (*a*) S. Fukuzumi, *Phys. Chem. Chem. Phys.*, 2008, **10**, 2283–2297; (*b*) A. Kira, T. Umeyama, Y. Matano, K. Yoshida, S. Isoda, J. K. Park, D. Kim and H. Imahori, *J. Am. Chem. Soc.*, 2009, **131**, 3198–3200; (*c*) Y. Hizume, K. Tashiro, R. Charvet, Y. Yamamoto, A. Saeki, S. Seki and T. Aida, *J. Am. Chem. Soc.*, 2010, **132**, 6628–6629.
8 D. M. Guldi, B. M. Illescas, C. M. Atienza, M. Wielopolskia and N. Martín, *Chem. Soc. Rev.*, 2009, **38**, 1587–1597.
9 P. Bhyrappa and K. Karunanithi, *Inorg. Chem.*, 2010, **49**, 8389–8400.
10 O. Ito and K. Yamanaka, *Bull. Chem. Soc. Jpn.*, 2009, **82**, 316–332.
11 S. S. Gayathri, M. Wielopolski, E. M. Pérez, G. Fernández, L. Sánchez, R. Viruela, E. Ortí, D. M. Guldi and N. Martín, *Angew. Chem., Int. Ed.*, 2009, **48**, 815–819.
12 C. Bucher, C. H. Devillers, J. C. Moutet, G. Royal and E. Saint-Aman, *Coord. Chem. Rev.*, 2009, **253**, 21–36.
13 E. M. Pérez and N. Martín, *Chem. Soc. Rev.*, 2008, **37**, 1512–1519.
14 Y. Araki and O. Ito, *J. Photochem. Photobiol., C*, 2008, **9**, 93–110.
15 D. Bonifazi, O. Enger and F. Diederich, *Chem. Soc. Rev.*, 2007, **36**, 390–414.
16 J. W. Verhoeven, *J. Photochem. Photobiol., C*, 2006, **7**, 40–60.
17 T. Kawase and H. Kurata, *Chem. Rev.*, 2006, **106**, 5250–5273.
18 F. D'Souza and O. Ito, *Coord. Chem. Rev.*, 2005, **249**, 1410–1422.
19 T. S. Balaban, *Acc. Chem. Res.*, 2005, **38**, 612–623.
20 M. E. El-Khouly, O. Ito, P. M. Smith and F. D'Souza, *J. Photochem. Photobiol., C*, 2004, **5**, 79–104.
21 M. D. Meijer, G. P. M. van Klink and G. van Koten, *Coord. Chem. Rev.*, 2002, **230**, 141–163.
22 H. Imahori, K. Hagiwara, T. Akiyama, M. Aoki, S. Taniguchi, T. Okada and M. Y. Sakata, *Chem. Phys. Lett.*, 1996, **263**, 545–550.
23 A. Hirsch, *Fullerenes and Related Structures*, vol. 199, Springer, Berlin, 1999, .
24 N. S. Sariciftci, L. Smilowitz, A. J. Heeger and F. Wudl, *Science*, 1992, **258**, 1474–1476.
25 M. Prato, *J. Mater. Chem.*, 1997, **7**, 1097–1109.
26 N. Martín, L. Sánchez, B. Illescas and I. Pérez, *Chem. Rev.*, 1998, **98**, 2527–2547.
27 S. Fukuzumi, I. Nakanishi, T. Suenobu and K. M. Kadish, *J. Am. Chem. Soc.*, 1999, **121**, 3468–3474.
28 D. M. Guldi, *Chem. Commun.*, 2000, 321–327.
29 D. M. Guldi and M. Prato, *Acc. Chem. Res.*, 2000, **33**, 695–703.
30 A. Hirsch and M. Bretteich, *Fullerenes: Chemistry and Reaction*, Wiley-VCH, Weinheim, 2005.
31 B. M. Illescas and N. Martín, *C. R. Chim.*, 2006, **9**, 1038–1050.
32 A. Mateo-Alonso, D. M. Guldi, F. Paolucci and M. Prato, *Angew. Chem., Int. Ed.*, 2007, **46**, 8120–8126.
33 (*a*) J. Deisenhofer, Academic Press, San Diego, 1993; (*b*) J. Diesenhofer and H. Michel, *Angew. Chem., Int. Ed. Engl.*, 1989, **28**, 829; (*c*) G. Feher, J. P. Allen, M. Y. Okamura and D. C. Rees, *Nature*, 1989, **339**, 111; (*d*) N. K. Subbaiyan, S. A. Wijesinghe and F. D'Souza, *J. Am. Chem. Soc.*, 2009, **131**, 14646–14647; (*e*) M. Fazio, O. P. Lee and D. I. Schuster, *Org. Lett.*, 2008, **10**, 4979–4982; (*f*) J. D. Megiatto, D. I. Schuster, S. Abwandner, G. de Miguel and D. M. Guldi, *J. Am. Chem. Soc.*, 2010, **132**, 3847–3861.
34 N. K. Subbaiyan, L. Obraztsov, C. A. Wijesinghe, K. Tran, W. Kutner and F. D'Souza, *J. Phys. Chem. C*, 2009, **113**, 8982–8989.
35 A. Kira, T. Umeyama, Y. Matano, K. Yoshida, S. Isoda, J. K. Park, D. Kim and H. Imahori, *J. Am. Chem. Soc.*, 2009, **131**, 3198.
36 J. F. Gnichwitz, M. Wielopolski, K. Hartnagel, U. Hartnagel, D. M. Guldi and A. Hirsch, *J. Am. Chem. Soc.*, 2008, **130**, 8491–8501.
37 A. Mateo-Alonso, C. Sooambar and M. Prato, *C. R. Chim.*, 2006, **9**, 944–951.
38 (*a*) F. D'Souza, M. E. El-Khouly, S. Gadde, A. L. McCarty, P. A. Karr, M. E. Zandler, Y. Araki and O. Ito, *J. Phys. Chem. B*, 2005, **109**, 10107–10114; (*b*) A. Mateo-Alonso, C. Ehli, D. M. Guldi and M. Prato, *J. Am. Chem. Soc.*, 2008, **130**, 14938–14939; (*c*) F. D'Souza, S. Gadde, M. E. Zandler, M. Itou, Y. Arakib and O. Ito, *Chem. Commun.*, 2004, 2276–2277.
39 J. Santos, B. Grimm, B. M. Illescas, D. M. Guldi and N. Martín, *Chem. Commun.*, 2008, 5993–5995.
40 F. Wessendorf, J. F. Gnichwitz, G. H. Sarova, K. Hager, U. Hartnagel, D. M. Guldi and A. Hirsch, *J. Am. Chem. Soc.*, 2007, **129**, 16057–16071.
41 J. L. Sessler, J. Jayawickramarajah, A. Gouloumis, T. Torres, D. M. Guldi, S. Maldonado and K. J. Stevenson, *Chem. Commun.*, 2005, 1892–1894.
42 P. Mukherjee, S. Bhattacharya, S. K. Nayak, S. Chattopadhyay and S. Bhattacharya, *Chem. Phys.*, 2009, **360**, 116–122.
43 V. Sgobba, G. Giancane, S. Conoci, S. Casilli, G. Ricciardi, D. M. Guldi, M. Prato and L. Valli, *J. Am. Chem. Soc.*, 2007, **129**, 3148–3156.
44 K. Okuda, C. Abeta, T. Hirota, M. Mochizuki and T. Mashino, *Chem. Pharm. Bull.*, 2002, **50**, 985–987.
45 Y. Ishikawa, A. Yamashita and T. Uno, *Chem. Pharm. Bull.*, 2001, **49**, 287–293.
46 F. Oswald, M. E. El-Khouly, Y. Araki, O. Ito and F. Langa, *J. Phys. Chem. B*, 2007, **111**, 4335–4341.
47 (*a*) F. D'Souza, G. R. Deviprasad, M. E. Zandler, V. T. Hoang, A. Klykov, M. VanStipdonk, A. Perera, M. E. El-Khouly, M. Fujitsuka and O. Ito, *J. Phys. Chem. A*, 2002, **106**, 3243–3252; (*b*) H. A. Benesi and J. H. Hildebrand, *J. Am. Chem. Soc.*, 1949, **71**, 2703–2707; (*c*) J. R. Lakowicz, *Principles of Fluorescence Spectroscopy*, Kluwer/Plenum, New York, 2nd edn, 1999.
48 (*a*) D. M. Guldi, A. Gouloumis, P. Vázquezb and T. Torres, *Chem. Commun.*, 2002, 2056–2057; (*b*) T. D. Ros, M. Prato, D. M. Guldi, M. Ruzzi and L. Pasimeni, *Chem.–Eur. J.*, 2001, **7**, 816–827.
49 F. D'Souza, G. R. Deviprasad, M. E. Zandler, M. E. El-Khouly, M. Fujitsuka and O. Ito, *J. Phys. Chem. B*, 2002, **106**, 4952–4962.
50 H. Imahori, M. E. El-Khouly, M. Fujitsuka, O. Ito, Y. Sakata and S. Fukuzumi, *J. Phys. Chem. A*, 2001, **105**, 325–332.
51 K. Wang, Y.-S. Wu, G.-T. Wang, R.-X. Wang, X.-K. Jiang, H.-B. Zhan and T. Li, *Tetrahedron*, 2009, **65**, 7718–7729.
52 (*a*) B. Delley, *J. Chem. Phys.*, 1990, **92**, 508–517; (*b*) B. Delley, *J. Chem. Phys.*, 2000, **113**, 7756–7764. *Dmol* is available as part of *Material Studio* and *Cerius2* by Accelrys Inc.